# Learned Interferometric Imaging for the SPIDER Instrument

Matthijs Mars, Marta M. Betcke, Jason D. McEwen

*Mullard Space Science Laboratory, University College London (UCL)*

## 1. SPIDER

The **Segmented Planar Imaging Detector for Electro-Optical (EO) Reconnaissance (SPIDER)** [1, 2] aims to be a smaller, lighter, cheaper and more power-efficient alternative to state-of-the-art space telescopes.

The interferometer measures 4440 visibilities (Fourier coefficients) given by

$$\hat{f}(\xi) = \int_{-\infty}^{\infty}\int_{-\infty}^{\infty} f(\chi)\, e^{-i2\pi\chi\cdot\xi} d\chi, \quad (1)$$

where Fourier coefficients $\hat{f}$ measured at non-uniformly distributed coordinates $\xi = (u, v)$ are calculated by the continuous Fourier transform of the signal $f$ measured at spatial coordinates $\chi$.

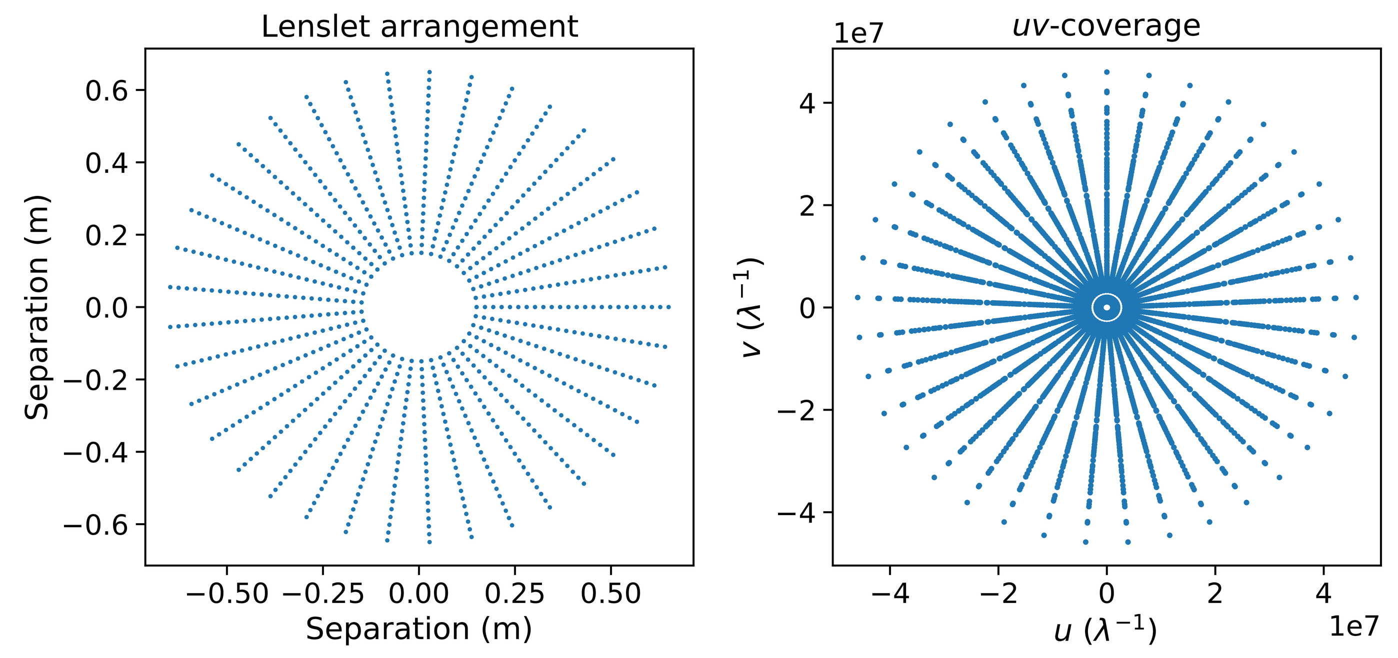


Figure: Arrangement of the lenslets of the SPIDER instrument (*left*) and the resulting Fourier sampling (*right*).

## 2. Interferometric Imaging Problem

The interferometric imaging problem can be concisely described as

$$\boldsymbol{y} = \Phi \boldsymbol{x} + \boldsymbol{n}, \quad (2)$$

- Non-uniformly distributed Fourier measurements, $\boldsymbol{y} \in \mathbb{C}^K$
- Measurement operator, $\Phi : \mathbb{R}^N \to \mathbb{C}^K$
- Image, $\boldsymbol{x} \in \mathbb{R}^N$
- Measurement noise, $\boldsymbol{n} \in \mathbb{C}^K$

The measurement operator is modelled using a **non-uniform fast Fourier Transform (NUFFT)** [3]:

$$\Phi = \boldsymbol{GFZD}, \quad (3)$$

- $\boldsymbol{G} : \mathbb{C}^{\alpha^2 N} \to \mathbb{C}^M$, Degridding operator
- $\boldsymbol{F} : \mathbb{C}^{\alpha^2 N} \to \mathbb{C}^{\alpha^2 N}$, Fast Fourier Transform
- $\boldsymbol{Z} : \mathbb{R}^N \to \mathbb{R}^{\alpha^2 N}$, Zero-padding
- $\boldsymbol{D} : \mathbb{R}^N \to \mathbb{R}^N$, Correction operator (corrects for effects induced by gridding)

Traditional reconstruction approaches use iterative solvers to find

$$\boldsymbol{x}^* = \underset{\boldsymbol{x} \in X}{\arg\min} \quad \|\Phi\boldsymbol{x} - \boldsymbol{y}\|_{\ell_2}^2 + \lambda\|\Psi^\dagger \boldsymbol{x}\|_{\ell_1}, \quad (4)$$

- $\mathcal{L} = \|\Phi\boldsymbol{x} - \boldsymbol{y}\|_{\ell_2}^2$, data fidelity term
- $\mathcal{S} = \|\Psi^\dagger \boldsymbol{x}\|_{\ell_1}$, sparsity prior, with $\Psi$ typically a dictionary of wavelet bases

Traditional approaches are

- Computationally expensive, because they evaluate the measurement operator every iteration
- Limited by the prior information captured in the handcrafted prior ($\mathcal{S}$)

## 3. Learned Interferometric Imaging [5]

To reduce computational cost and get increased reconstruction quality through data-driven priors, we use two learned imaging approaches:

**Learned post-processing**

- $\boldsymbol{x}^* = \Phi_\theta^\dagger \boldsymbol{y} = \Lambda_\theta \Phi^\dagger \boldsymbol{y}$, with $\Lambda_\theta$ a learned correction operator
- Using a **U-Net** denoiser [6]
- Computationally efficient since it only evaluates the measurement operator once
- Limited performance dependent on the amount of information captured by the pseudo-inverse

**Unrolled Iterative**

- Mimic traditional iterative solvers
- Train a few unrolled iterations of an iterative optimization algorithm
- Computationally less expensive than iterative solvers as it typically needs fewer (unrolled) iterations
- Better reconstruction quality through data-driven priors and leveraging the measurement operator in the reconstruction process

Our unrolled iterative approach uses a **Gradient U-Net (GU-net)** which is a modified U-Net where at each resolution scale we add information captured by the measurement operator. For this we need **sub-scale measurement operators** $\Phi_i : \mathbb{R}^{N_i} \to \mathbb{C}^{K_i}$, that:

- Are applied at a reduced image scale (through down-sampling in the U-Net)
- Work on a restricted Fourier space through applying a low-pass filter to the Fourier measurements
- Are computationally inexpensive since they work on a reduced image and Fourier space

Using these we can calculate the update based on measurement information added at each scale $i$:

$$\tilde{\boldsymbol{x}}_i = \Lambda_{i,\theta}(\boldsymbol{x}_i,\ \nabla_{\boldsymbol{x}_i}\mathcal{L}(\Phi_i \boldsymbol{x}_i,\ \boldsymbol{y}_i), \nabla^f_{\boldsymbol{x}_i}\mathcal{L}(\Phi_i \boldsymbol{x}_i,\ \boldsymbol{y}_i), \Phi_i^* \boldsymbol{y}_i). \quad (5)$$

- $\boldsymbol{x}_i$, the first channel at scale $i$
- $\nabla_{\boldsymbol{x}_i}\mathcal{L}(\Phi_i \boldsymbol{x}_i,\ \boldsymbol{y}_i)$, the gradient of the data-fidelity term
- $\nabla^f_{\boldsymbol{x}_i}\mathcal{L}(\Phi_i \boldsymbol{x}_i,\ \boldsymbol{y}_i)$, the **filtered** gradient of the data-fidelity term
- $\Phi_i^* \boldsymbol{y}_i$, the scale-restricted dirty reconstruction

## GU-Net architecture

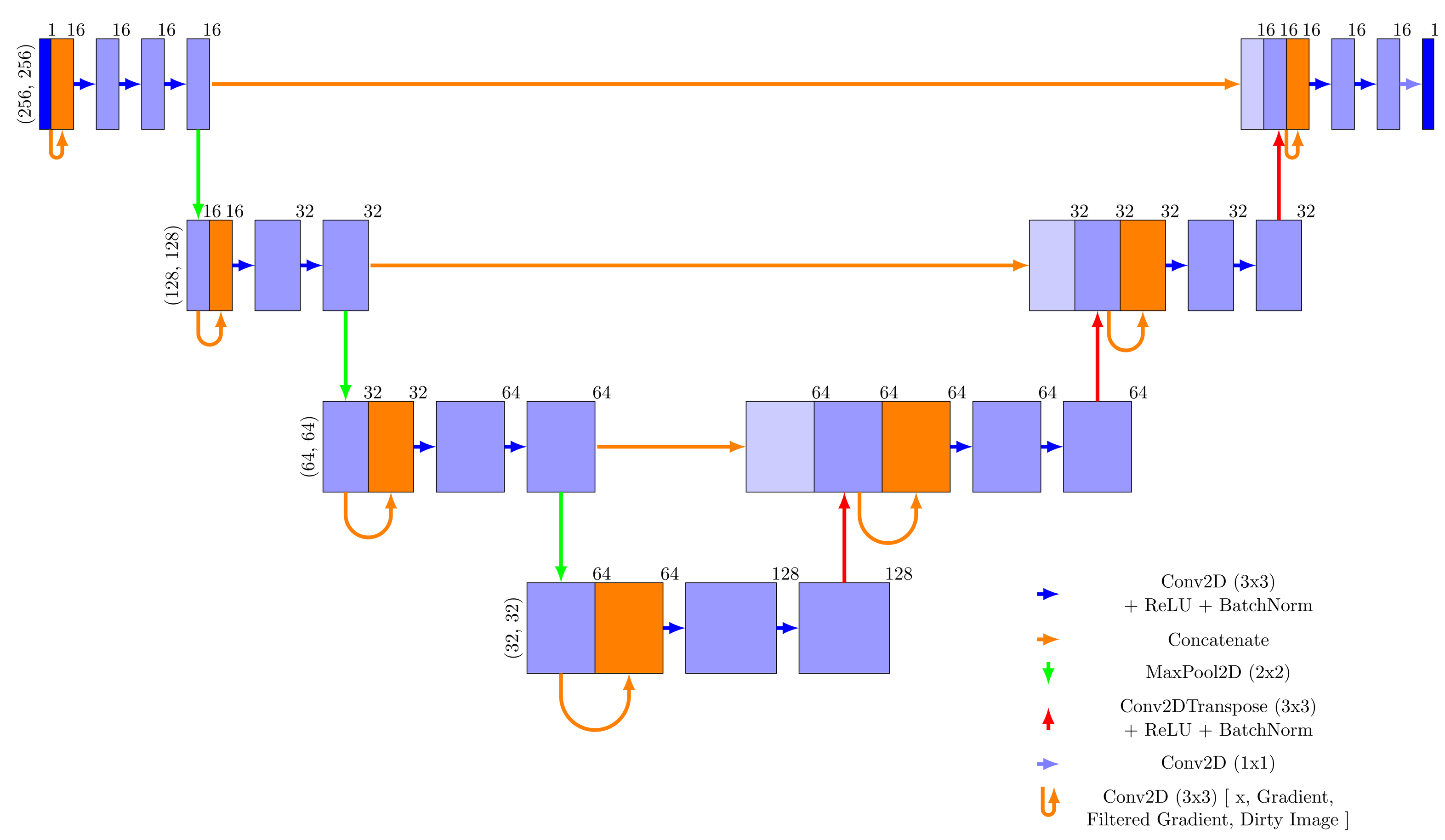


## 4. Experiment

Simulating measurements from 256 × 256 images using the NUFFT with 30dB ISNR Gaussian noise. Using the simulated measurements we perform two experiments

**1:** Test performance on large dataset of natural images

- images from the **COCO dataset** [8] (2000 train, 1000 test)
- Train for 200 epochs on the ADAM optimizer, a learning rate of 0.001, and a batch size of 5

**2:** Test performance on small, domain-specific datasets
Using transfer learning from the models trained on natural images to repurpose the models to the following two datasets (300 train, 150 test):

- Galaxy simulations from **IllustrisTNG simulations** [9]
- Satellite images from **Deep Globe satellite challenge** [10]

## References

[1] Kendrick et al. 2013, "Segmented Planar Imaging Detector for EO Reconnaissance"

[2] Duncan et al. 2015, "SPIDER: Next generation chip scale imaging sensor"

[3] Dutt & Rohklin 1993, "Fast Fourier Transforms for Nonequispaced Data"

[4] Pratley et al. 2018, "Robust Sparse Image Reconstruction of Radio Interferometric Observations with Purify"

[5] Mars et al. 2023, "Learned Interferometric Imaging for the SPIDER Instrument"

[6] Ronneberger et al. 2015, "U-Net: Convolutional Networks for Biomedical Image Segmentation"

[7] Pan & Betcke 2022, "On Learning the Invisible in Photoacoustic Tomography with Flat Directionally Sensitive Detector"

[8] Lin et al. 2014, "Microsoft COCO: Common Objects in Context"

[9] Nelson et al. 2019, "The IllustrisTNG Simulations: Public Data Release"

[10] Demir et al. 2018, "DeepGlobe 2018: A Challenge to Parse the Earth through Satellite Images"

## 5. Results

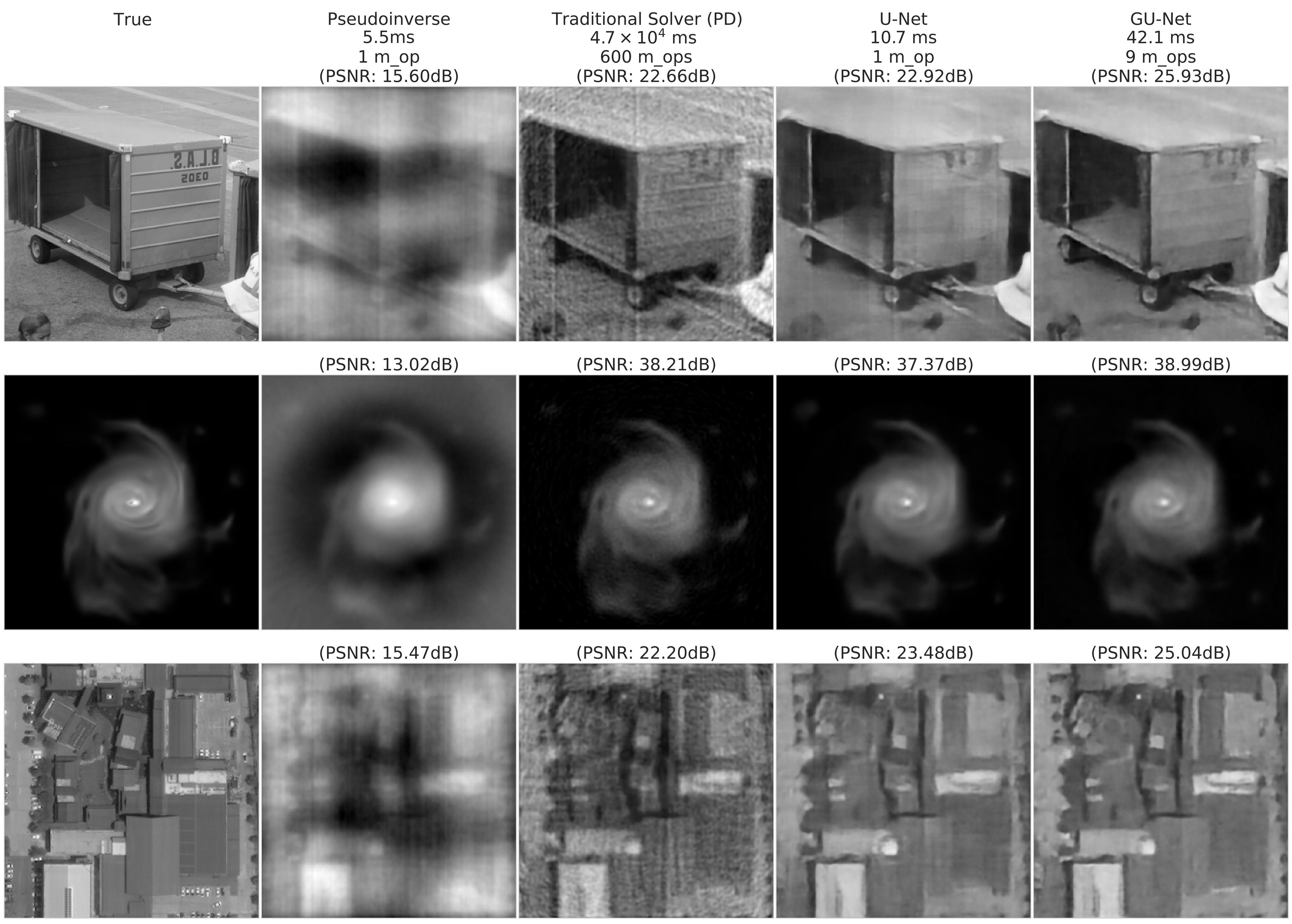


Figure: Reconstructions and the computation time, number of (full-scale) measurement operator evaluations (m_ops), and peak signal-to-noise ratio (PSNR) of the reconstructions for the COCO (top), IllustrisTNG (middle), and Deep Globe datasets.

E-mail: matthijs.mars.20@ucl.ac.uk

Paper: https://arxiv.org/abs/2301.10260